Design Trade-offs in Feed Systems for Ultra-wideband VLBI Observations

Jonas Flygare, Miroslav Pantaleev, John Conway, Michael Lindqvist, Rüdiger Haas

Abstract Due to the advanced capability of today's ultra-wideband feed systems and low-noise amplifiers, interesting upgrades for future VLBI receiver and telescope design should be considered. Multiple input parameters need to be taken into account for optimal sensitivity and applications of the future astronomical and geodetic observational systems. In this paper we present an overview of some trade-offs for wideband systems between SEFD, bandwidth, and telescope reflector optics. We evaluate receiver bandwidths from 3.5:1 to 10.3:1 bandwidth within the frequency range 1.5–24 GHz in different configurations. Due to potential RFI pollution of the lower frequencies we present potential feed upgrades for the most common reflector geometries of VGOS and EVN telescopes that mitigate this problem. The results of this work is relevant for future VLBI stations and telescope design in general.

Keywords SEFD, VLBI, ultra wideband, VGOS, Quad-Ridge Flared Horn

1 Introduction

The VLBI Global Observing System (VGOS) network typically uses frequencies over 2–18 GHz with receiver bandwidth ratios of 6:1. The benefit of wideband feed systems is that continuous observational bandwidth will be available, at the expense of absolute system equivalent flux density (SEFD) over frequency. Despite this trade-off, with current state-of-the-art low-noise amplifiers (LNA) and highly optimized feed antennas, a good sensitivity (SEFD) level can still be achieved.

Onsala Space Observatory: Department of Space, Earth and Environment, Chalmers University of Technology, S-43992, Onsala, Sweden.
Email: jonas.flygare@chalmers.se

Fig. 1 Onsala Twin Telescope (OTT) on the left and center; Onsala 25-m telescope on the right.

The research project BRoad-bAND (BRAND), funded by EU Horizon 2020 RadioNet, will cover a decade in frequency over 1.5–15.5 GHz with a single-pixel feed [1]. This receiver system will enable continuous observations within the European VLBI Network (EVN) over L-, S-, C-, X-, and Ku-band. We evaluate the BRAND feed with simulations in a VGOS reflector, the Onsala Twin Telescope (OTT) [2], see Figure 1, and compare to the current system installed on one of the telscopes [3]. Due to the radio frequency interference (RFI) pollution at L- and S-band frequencies and the probable release of more frequencies for 5G telecommunication, potential new frequency bands should also be investigated. With respect to this, we present the high-frequency quad-ridge flared horn (QRFH) developed for the Square Kilometre Array (SKA) project covering 4.6–24 GHz [4] and evaluate it in the VGOS reflector through simulations. These feeds are optimized for reflectors with low focal length

over diameter ratio, f/D, which corresponds to a large half-subtended opening angle, θ_e, see Figure 2. Since many of the EVN telescopes are reflectors with high f/D, we include a feed system over 4.4–15.5 GHz designed for the Onsala 20-m telescope to compare. In this paper we use measured feed beam patterns for the current OTT QRFH over 3–18 GHz and for the SKA Band B QRFH over 4.6–24 GHz. The feed beam patterns for the BRAND QRFH over 1.5–15.5 GHz and the 4.4–15.5 GHz system for Onsala 20-m telescope are simulated. The measured patterns show good agreement with simulated. The patterns are used in the system simulator for the full telescope beam pattern simulations described in the next section.

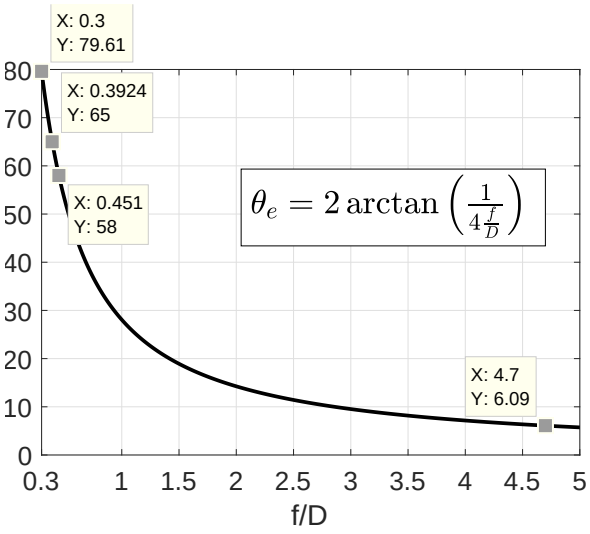

Fig. 2 Half-subtended angle θ_e seen from the feed-point, plotted against corresponding effective f/D for the reflector geometry.

2 Analysis

In the analysis we compare four different reflector geometries that are illustrated in Figure 3. The corresponding θ_e are highlighted in Figure 2 with the largest being $\theta_e = 79.61^\circ$ for the prime-focus reflector and the Cassegrain dual-reflector the smallest $\theta_e = 6.09^\circ$. The Gregorian ring-focus (VGOS) represents $\theta_e = 65^\circ$ and the Gregorian offset $\theta_e = 58^\circ$.

For accurate SEFD analysis we use a full system simulator [5] that uses physical optics (PO) + physical

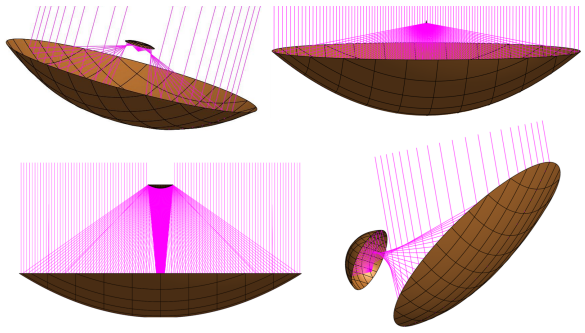

Fig. 3 (Top-left) Gregorian ring-focus axial-symmetric dual-reflector, common concept for VGOS; (Top-right) Primary-focus axial-symmetric reflector; (Bot-left) Cassegrain axial-symmetric dual-reflector, common concept within EVN; (Bot-right) Gregorian offset dual-reflector, common concept for new generation astronomy arrays (e.g., SKA, ngVLA).

theory of diffraction (PTD) to calculate the full telescope beam pattern, $G(\theta,\phi,f)$. The telescope reflector is fed with either simulated or measured feed beam patterns. The full telescope beam pattern is used to weight the surrounding sky noise temperature, $T(\theta,\phi,f)$, in a full-sphere integration to calculate the antenna noise temperature, T_A, see Equation 1. One key component in T_A is the amount of spill-over noise picked up from the 300 K ground noise temperature.

$$T_A = \frac{\int\int_{4\pi} G(\theta,\phi,f)T(\theta,\phi,f)\sin\theta\,\mathrm{d}\theta\,\mathrm{d}\phi}{\int\int_{4\pi} G(\theta,\phi,f)\sin\theta\,\mathrm{d}\theta\,\mathrm{d}\phi}. \quad (1)$$

For the feed models analyzed in this paper a very high radiation efficiency is achieved. Therefore we assume a simple model for the total system noise: $T_{sys} = T_A + T_{REC}$. T_{REC} represents the noise of the complete receiver chain. In Figure 4 we present two different re-

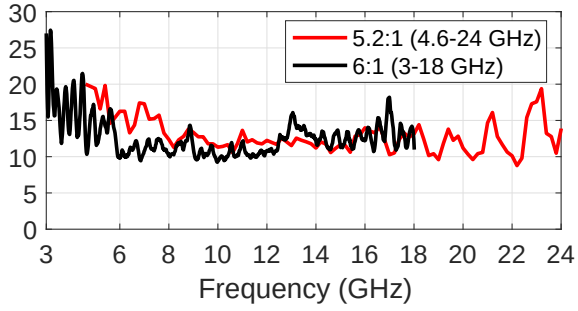

Fig. 4 Measured receiver noise temperatures, T_{REC}, for two different wideband systems in Onsala.

ceiver setups measured with Y-factor tests in Onsala that show good noise performance over wide frequency bandwidth.

From the telescope main-beam gain, G, we can calculate the effective area of the reflector as $A_{eff} = (G\lambda^2)/(4\pi)$. Finally, it is straightforward to calculate SEFD according to

$$SEFD = \frac{2k_B T_{sys}}{A_{eff}}, \quad (2)$$

where k_B is the Boltzmann constant. For accurate estimation we include appropriate degradation of SEFD due to the aperture blockage for the respective reflector geometry (not applicable for offset reflectors).

3 Wideband System Performance

In Figure 5 we present simulated aperture efficiency, $\eta_a = A_{eff}/A_{phy}$, of the receiver systems on different reflectors. A_{phy} is the available physical area of the reflector. The 10.3:1 feed was successfully designed for the prime-focus configuration with a challenging $\theta_e = 79.61°$ to illuminate. Therefore, in the VGOS reflector at the low-frequency end it is over-illuminating (lower η_a) but matches better at high frequency when the feed beamwidth is slightly narrowed. The 5.2:1 feed show fairly smooth η_a over bandwidth in the VGOS reflector. In Figure 6 we present the simulated SEFD at elevation $\theta = 30°$ for the wideband systems applicable to the VGOS reflector. Simulation of one of the current OTT receivers is represented with the green dash-dotted line over 3–18 GHz. An alternative 5.2:1 system is presented over 3.5–18 GHz for a possible mitigation of RFI below the 3.5 GHz. Due to the waveguide structure of the QRFH feed, it acts as a high-pass filter for frequencies below the cut-off. The receiver systems show excellent simulated SEFD performance where the ones with less than decade bandwidth show SEFD better than 1,000 Jy over most of the respective frequency band.

Another interesting aspect of these receiver systems is how the performance scales with size of the main reflector. Within the EVN, main-reflector diameters range up to 100 m. The OTT VGOS reflector measures 13.2 m, whilst the SKA offset Gregorian reflector is 15 m in effective diameter. SEFD scales inversely

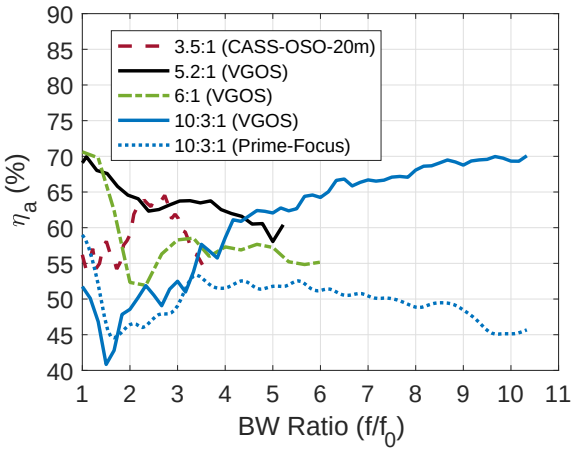

Fig. 5 Simulated aperture efficiency for different receiver systems in different reflector geometries. The bandwidth is normalized to the lowest frequency f_0.

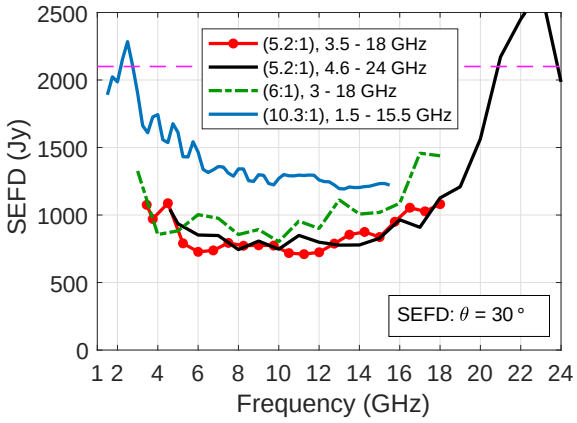

Fig. 6 Simulated SEFD for four different receiver systems in the OTT 13.2-m reflector (VGOS). Elevation: $\theta = 30°$, purple-dashed line represents the 2,100 Jy specification.

proportional to $A_{eff} = \eta_a A_{phy}$ (Equation 2). The physical main-reflector area can be written $A_{phy} = \pi(D_m/2)^2$ where D_m is the main-reflector diameter. In Figure 7 and Figure 8 we present SEFD as a contour plot over frequency and telescope main-reflector diameter, for the different receiver systems on different reflectors. The homogeneously dark red colored area represents SEFD higher than 2,100 Jy and does not fulfill VGOS specifications. For the VGOS type reflector in Figure 7 the 4.6–24 GHz system is on equal or better than the 3–18 GHz receiver on OTT, for overlapping frequencies. As mentioned, the higher cut-off frequency at 4.6 GHz mititgates potential LNA saturation from

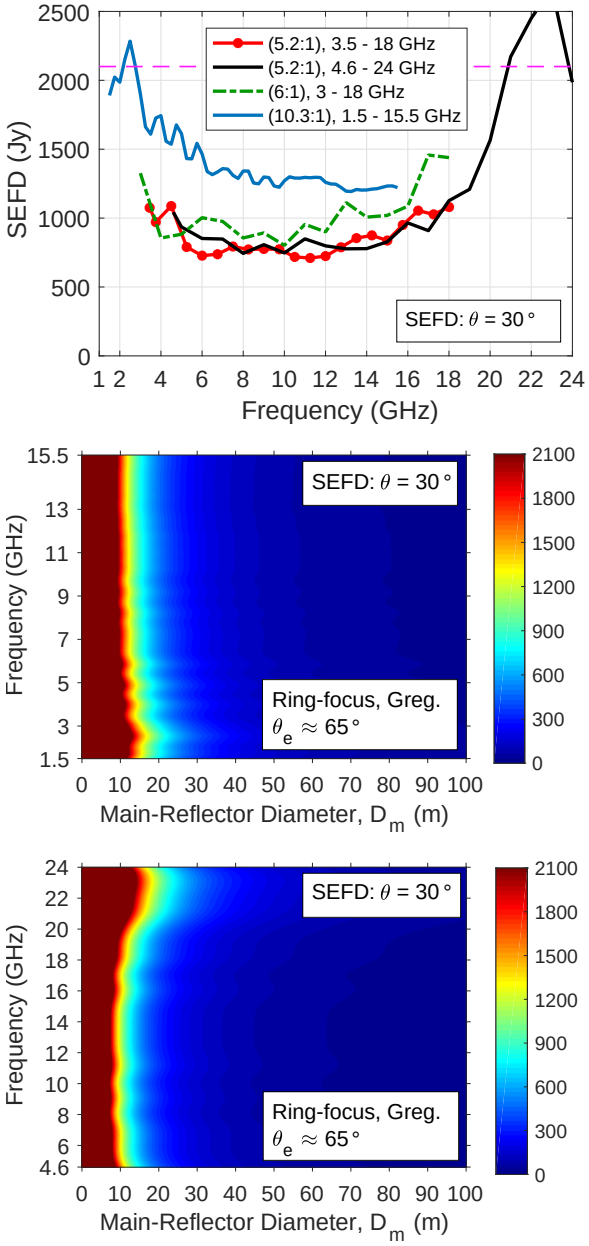

Fig. 7 Simulated SEFD (contour) for three receiver systems evaluated in Gregorian ring-focus type reflector (VGOS), plotted against main-reflector diameter size (x-axis) and frequency (y-axis). (Top) Current OTT, 6:1 bandwidth, 3–18 GHz; (Mid) BRAND, 10.3:1 bandwidth, 1.5–15.5 GHz; (Bot.) SKA Band B, 5.2:1, 4.6–24 GHz.

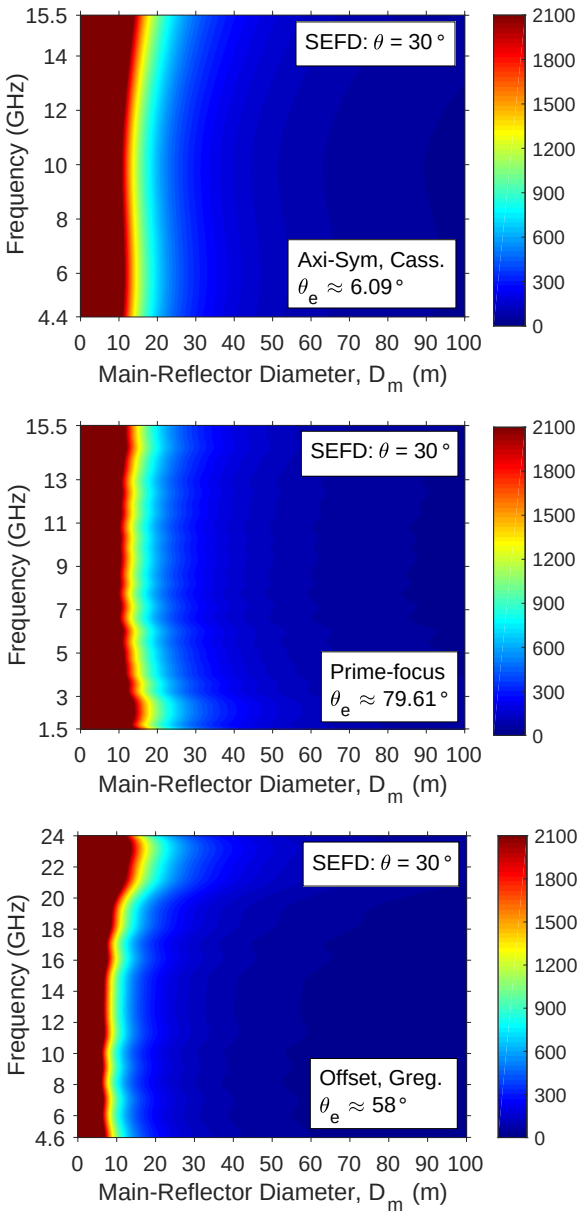

Fig. 8 Simulated SEFD (contour) for three receiver systems evaluated in three different reflector types, plotted against main-reflector diameter size (x-axis) and frequency (y-axis). (Top) Cassegrain dual-reflector, wideband system, 3.5:1 bandwidth, 4.4–15.5 GHz; (Mid) Prime-focus reflector, BRAND, 10.3:1 bandwidth, 1.5–15.5 GHz; (Bot.) Shaped Offset Gregorian reflector, SKA Band B, 5.2:1, 4.6–24 GHz.

the lower bands whilst the inclusion of the water-line at 22 GHz within the band introduces another possibility. In [6] we investigate theoretically this receiver system as a potential line-of-sight water vapor radiometer on the telescope. From simulation results, we expect a performance close to that of the dedicated water vapor radiometers of today. The obvious benefit is to have accurate water vapor measurements in the telescope line-

of-sight during observations with no separate system needed.

In general the receiver systems simulate better than specification on reflector diameters of 10–13 m for the Gregorian ring-focus type used in VGOS. The 1.5–15.5 GHz system can achieve similar SEFD for a 15-m dish in both Gregorian ring-focus and prime-focus reflectors, see middle plot in Figures 7 and 8, respectively. The best SEFD using the smallest reflector diameter is found in the highly shaped offset Gregorian reflector in the bottom row of Figure 8. This is expected as the feed is optimized specifically for this low-spillover reflector. For the Cassegrain dual-reflector system shown in the top row of Figure 8 the required reflector diameter is larger to achieve the same SEFD. This is due to the difficulty in designing feeds for a small θ_e over a large bandwidth without sacrificing aperture efficiency η_a. This type of feed in a standard horn configuration generally needs to be very large, which makes it difficult to fit in the receiver cabin as well. However, this result shows good performance over the 3.5:1 bandwidth which overlaps with VGOS frequencies. This configuration also has a higher cut-off frequency to mitigate low-frequency RFI pollution and is suitable for reflectors with small θ_e, which is common within the EVN. The frequency band available would allow for joint VLBI observations with VGOS.

4 Conclusions

We present different receiver systems applicable especially to the VGOS-type Gregorian ring-focus reflector. The presented receiver systems are evaluated through simulation with respect to main-reflector diameter and bandwidth for VGOS and other common reflector geometries. The 4.6–24 GHz allows for an interesting upgrade option in future VGOS receivers with a less RFI-polluted frequency band. SEFD performance can be expected in the same order as current VGOS systems, with the possibility of line-of-sight WVR in parallel with observation (further studied in [6]). A receiver system overlapping VGOS frequencies and suitable for Cassegrain dual-reflectors with high f/D (e.g., EVN) was also presented and evaluated. Finally we include the 10.3:1 receiver developed for radio astronomy (BRAND) over 1.5–15.5 GHz. This option enables a decade in available bandwidth with a substantial overlap with VGOS frequencies, further enabling joint observations between these systems.

Acknowledgements

The authors thank the ÅForsk Foundation for funding a travel grant for Jonas Flygare to attend the IVS 2018 conference and presenting this work.

References

1. J. Flygare, M. Pantaleev, and S. Olvhammar, “BRAND: Ultra-Wideband Feed Development for the European VLBI Network - A Dielectrically Loaded Decade Bandwidth Quad-Ridge Flared Horn” in *Proc. 12th Euro. Conf. Antennas Propag. (EuCAP2018)*, London, UK, April 2018.
2. G. Elgered, R. Haas, J. Conway, R. Hammargren, L. Helldner, T. Hobiger, M. Pantaleev, L. Wennerbäck, “The Onsala Twin Telescopes Project” in *Proc. 23rd EVGA Working Meeting (EVGA2017)*, Gothenburg, Sweden, May 2017.
3. J. Flygare, M. Pantaleev, B. Billade, M. Dahlgren, L. Helldner, and R. Haas, “Sensitivity and antenna noise temperature analysis of the feed system for the Onsala twin telescopes” in *Proc. 23rd EVGA Working Meeting (EVGA2017)*, Gothenburg, Sweden, May 2017.
4. B. Dong, J. Yang, J. Dahlström, J. Flygare, M. Pantaleev, and B. Billade, “Optimization and Realization of Quadruple-ridge Flared Horn with New Spline-defined Profiles as a High-efficiency Feed for Reflectors over 4.6-24 GHz”, *IEEE Trans. Antennas. Propag.*, August 2017 (accepted for publ.).
5. M. V. Ivashina, O. Iupikov, R. Maaskant, W. A. Van Cappellen, and T. Oosterloo, “An optimal beamforming strategy for wide-field surveys with phased-array-fed reflector antennas” in *IEEE Trans. Antennas Propag.,* vol. 59, no. 6, pp. 1864-1875, 2011.
6. J. Flygare, M. Pantaleev, J. Conway, M. Lindqvist, L. Helldner, M. Dahlgren, R. Haas, and P. Forkman, “Ultra-wideband feed systems for the EVN and SKA - evaluated for VGOS” in *Proc. 10th Int. VLBI Service for Geodesy and Astrometry (IVS) General Meeting*, Longyearbyen, Svalbard/Norway, June, 2018.